

Formations of Mixed-Valence Oxovanadium^{V,IV} Citrates and Homocitrate with N-Heterocycle Chelated Ligand

Can-Yu Chen, Zhao-Hui Zhou,* Hong-Bin Chen, Pei-Qiang Huang, Khi-Rui Tsai, and Yuan L. Chow

State Key Laboratory of Physical Chemistry of Solid Surfaces and Department of Chemistry, College of Chemistry and Chemical Engineering, Xiamen University, Xiamen, 361005, China

Received March 27, 2008

Dimeric mixed-valence oxovanadium citrate $[V_2O_3(\text{phen})_3(\text{Hcit})] \cdot 5H_2O$ (**1**) ($H_4\text{cit}$ = citric acid, phen = 1,10-phenanthroline) was isolated from a weak acidic medium. It could be converted quantitatively into a tetrameric oxovanadium citrate adduct of 1,10-phenanthroline $[V_2O_3(\text{phen})_3(\text{Hcit})_2(\text{phen})_3O_3V_2] \cdot 12H_2O$ (**2**). This was supported by the trace of infrared spectra and X-ray diffraction patterns. The two compounds feature a bidentate citrate group that chelates only to one vanadium center through their negatively charged α -alkoxy and α -carboxy oxygen atoms, while the other β -carboxy and β -carboxylic acid groups are free to participate in strong intramolecular and intermolecular hydrogen bonding [2.45(1) in **1** and 2.487(2) Å in **2**], respectively. This is also the case of homocitrato vanadate(V/IV) $[V_2O_3(\text{phen})_3(R,S\text{-}H_2\text{homocit})]Cl \cdot 6H_2O$ (**3**) ($H_4\text{homocit}$ = homocitric acid), which features a binding mode similar to that found in the *R*-homocitrato iron molybdenum cofactor of Mo-nitrogenase. Moreover, the homocitrato vanadate(V) $[VO_2(\text{phen})_2]_2[V_2O_4(R,S\text{-}H_2\text{homocit})_2] \cdot 4H_2O \cdot 2C_2H_5OH$ (**4**) is isolated as a molecular precursor for the formation of mixed-valence complex **3**. The $V-O_{\alpha\text{-alkoxy}}$ and $V-O_{\alpha\text{-carboxy}}$ bond distances of homocitrato complexes **3** and **4** are 1.858(4) and 1.968(6)_{av} and 2.085(4) and 1.937(5) Å, respectively. They are shorter than those of homocitrate to FeVco (2.15 Å). The γ -carboxy groups of coordinated homocitrato complexes **3** and **4**, and the free homocitrate salt $Na_3(H\text{homocit}) \cdot H_2O$ (**5**), form strong hydrogen bonds with the chloride ion and the water molecule [2.982(5) in **3**, 2.562(9) in **4**, and 2.763(1) Å in **5**], respectively.

Introduction

Detailed crystallographic analysis of nitrogenase has revealed a previously unrecognized light atom in the center of six iron atoms of the *R*-homocitrato-MoFe₇S₉X (FeMoco) cluster,¹ which is supported by the theoretical study and model compound synthesis of iron sulfur clusters with similar cores of Fe₈S₉ and Fe₈S₈N, as well as analyses of ⁵⁷Fe nuclear resonance vibrational spectroscopy data.^{2–4} This idea has been expanded, and it is now believed that iron-centered vanadium cofactor (FeVco) has a very similar chemical

environment to that of FeMoco.⁵ On the other hand, nitrogenase having a citrate in the place of homocitrate manifests itself with a weaker reduction of N₂, while the citrate analogue retains C₂H₂ reduction activity comparable to that of the wild type.^{6–8} It is proposed that homocitrate may facilitate the binding of the dinitrogen molecule through the dissociation of the bound α -carboxy

* Author to whom correspondence should be addressed. Phone: +86 592 2184531. Fax: +86 592 2183047. E-mail address: zhzhou@xmu.edu.cn.

- (1) (a) Einsle, O.; Tezcan, F. A.; Andrade, S. L. A.; Schmid, B.; Yoshida, M.; Howard, J. B.; Rees, D. C. *Science* **2002**, *297*, 1696–1700. (b) Howard, J. B.; Rees, D. C. *Proc. Natl. Acad. Sci. U. S. A.* **2006**, *103*, 17088–17093.
- (2) Hinnemann, B.; Nørskov, J. K. *J. Am. Chem. Soc.* **2003**, *125*, 1466–1467.
- (3) Ohhi, Y.; Ikagama, Y.; Tatsumi, K. *J. Am. Chem. Soc.* **2007**, *297*, 10457–10465.
- (4) Xiao, Y.; Fischer, K.; Smith, M. C.; Newton, W.; Case, D. A.; George, S. J.; Wang, H.; Sturhahn, W.; Alp, E. E.; Zhao, J.; Yoda, Y.; Cramer, S. P. *J. Am. Chem. Soc.* **2006**, *128*, 7608–7612.

- (5) (a) Hales, B. J.; Case, E. E.; Morningstar, J. E.; Dzeda, M. F.; Mauterer, L. A. *Biochemistry* **1986**, *25*, 7251–7264. (b) Strange, R. W.; Eady, R. R.; Lawson, D.; Hasnain, S. S. *J. Synchrotron Radiat.* **2003**, *10*, 71–75.
- (6) (a) Hoover, T. R.; Robertson, A. D.; Cerny, R. L.; Hayes, R. N.; Imperial, J.; Shah, V. K.; Ludden, P. W. *Nature* **1987**, *329*, 855–857. (b) Hoover, T. R.; Imperial, J.; Ludden, P. W.; Shah, V. K. *Biochemistry* **1989**, *28*, 2768–2771.
- (7) (a) Imperial, J.; Hoover, T. R.; Madden, M. S.; Ludden, P. W.; Shah, V. K. *Biochemistry* **1989**, *28*, 7796–7799. (b) Mayer, S. M.; Gormal, C. A.; Smith, B. E.; Lawson, D. M. *J. Biol. Chem.* **2002**, *277*, 35263–35266.
- (8) (a) Burgess, B. K. *Chem. Rev.* **1990**, *90*, 1377–1406. (b) Ludden, P. W.; Shah, V. K.; Roberts, G. P.; Homer, M.; Allen, R.; Paustian, T.; Roll, J.; Chatterjee, R.; Madden, M.; Allen, J. *ACS Symp. Ser.* **1993**, *535*, 196–215.

or α -alkoxy groups from the Mo atom,^{9,10} and also the formation of an intramolecular hydrogen bond.¹¹ In the previous study, our investigations have addressed the coordination chemistry of citrate or homocitrate vanadium and molybdenum complexes.^{12–16} In order to understand the interaction of tricarboxylate ligands with vanadium in detail, the binding of citrates is now extended to mixed-valence citrate and homocitrate vanadium systems; this is reported in this paper.

Experimental Section

Physical Measurements. The pH value was measured by a potentiometric method with a digital PHB-8 pH meter. Infrared spectra were recorded as Nujol mulls in KBr plates on a Nicolet 360 FT-IR spectrometer. Elemental analyses were performed with an EA 1100 elemental analyzer. The electronic spectra were recorded on a Shimadzu UV 2501 spectrophotometer with an integrating sphere for reflectance spectroscopy. X-ray photoelectron spectra (XPS) were recorded on a Quantum 2000 Scanning ESCA Microprobe electron spectrometer using Al K α radiation with a pass energy of 46.95 eV. The binding energy (BE) scale was regulated by setting the C 1s transition at 284.6 eV (accuracy of BE was ± 0.1 eV). Electron paramagnetic resonance (EPR) spectra of compounds were collected at different temperatures on a Bruker EMX-10/12 spectrometer. X-ray diffraction (XRD) patterns were recorded on a Philips X'Pert Pro Super X-ray diffractometer equipped with X'Celerator and Xe detection systems. ¹³C NMR spectra were recorded in D₂O on a Bruker AV400 NMR spectrometer using sodium 2,2-dimethyl-2-silapentane-5-sulfonate as an internal reference.

Preparations of [V₂O₃(phen)₃(Hcit)]·5H₂O (1) and [V₂O₃(phen)₃(Hcit)₂(phen)₂O₃V₂]·12H₂O (2). Vanadium pentoxide (0.55 g, 3.0 mmol) dissolved in 2 mol L⁻¹ of potassium hydroxide (5.0 mL) was mixed with citric acid monohydrate (1.91 g, 9.1 mmol) solution in 100 mL of water. 1,10-Phenanthroline monohydrate (0.61 g, 3.1 mmol) in 95% ethanol (50 mL) was added, and the resulting mixture was brought to pH 4.0 with a potassium hydroxide solution. The dark green solution was set aside for two weeks to deposit crystals that were collected and washed with ethanol to afford **1** (0.81 g, 81% yield based on phenanthroline). Found (calcd for C₄₂H₃₉N₆O₁₅V₂): C, 51.7 (52.0); H, 4.2 (4.1); N, 8.5 (8.7%). IR (KBr, cm⁻¹): $\nu_{\text{as}}(\text{COO})$, 1627_{vs}; $\nu_{\text{s}}(\text{COO})$, 1427_s, 1385_w, 1342_w; $\nu(\text{V}=\text{O})$, 965_m, 936_m; $\nu(\text{V}-\text{O}-\text{V})$, 851_s. A similar procedure was used except that the final pH was adjusted to 5.1 to obtain **2**. Vanadium pentoxide (90.0 mg, 0.50 mmol) dissolved in 2 mol L⁻¹

of potassium hydroxide solution was mixed with a solution of citric acid monohydrate (0.22 g, 1.02 mmol) and 1,10-phenanthroline monohydrate (0.20 g, 1.02 mmol) in 25 mL of water–ethanol (2:1 by volume). The mixture was brought to pH 5.1 with a potassium hydroxide solution. The dark green crystals were isolated as **2** (0.13 g, 50% yield based on phenanthroline). Found (calcd for C₈₄H₈₂N₁₂O₃₂V₄): C, 51.3 (51.1); H, 4.3 (4.2); N, 8.6 (8.5%). IR (KBr, cm⁻¹): $\nu_{\text{as}}(\text{COO})$, 1625_{vs}; $\nu_{\text{s}}(\text{COO})$, 1426_s, 1385_w, 1344_w; $\nu(\text{V}=\text{O})$, 961_m, 936_m; $\nu(\text{V}-\text{O}-\text{V})$, 853_s.

Preparation of [V₂O₃(phen)₃(R,S-H₂homocit)]Cl·6H₂O (3). Homocitric acid γ -lactone (38.2 mg, 0.20 mmol) prepared according to the published method¹⁷ was dissolved in 4 mL of a potassium hydroxide solution (1.0 mol L⁻¹) at pH 11 with stirring, to which a solution (4 mL) of potassium vanadate (27.6 mg, 0.20 mmol) and an ethanol solution (3 mL) of 1,10-phenanthroline monohydrate (74.5 mg, 0.37 mmol) were added. The pH value of the mixture was brought to 2.5 by adding diluted HCl. The color changed to light yellow-green. The mixture was set aside to evaporate slowly for two weeks. The precipitate was filtered and washed with ethanol to afford dark green crystals (54.0 mg, 51% based on vanadium). Found (calcd for C₄₃H₄₄Cl₁N₆O₁₆V₂): C, 50.0 (49.7); H, 4.1 (4.3); N, 8.0 (8.1%). IR (KBr, cm⁻¹): $\nu(\text{COOH})$, 1720_s; $\nu_{\text{as}}(\text{COO})$, 1607_{vs}; $\nu_{\text{s}}(\text{COO})$, 1425_s, 1383_w, 1346_{vw}; $\nu(\text{V}=\text{O})$, 974_m, 941_m; $\nu(\text{V}-\text{O}-\text{V})$, 851_s. In the synthesis of **3**, [VO₂(phen)₂]₂[V₂O₄(R,S-H₂homocit)₂]·4H₂O·2C₂H₅OH (**4**) could be obtained in small amounts (yield ~5%) as a yellow solid, which redissolved to form **3** as the final product.

Preparation of Racemic Homocitrate Salt Na₃(Hhomocit)·H₂O (5). Racemic homocitric acid γ -lactone (107 mg, 0.57 mmol) prepared according to the published method¹⁷ was dissolved in 2.0 mol L⁻¹ of sodium hydroxide solution to a pH of 10.6 with stirring. The solution was hydrolyzed for 2 days at room temperature. The colorless product of racemic homocitrate salt **5** was obtained after one week of standing in a refrigerator. The yield of **5** was 85 mg (51%). Found (calcd for C₇H₉O₈Na₃): C, 28.8 (29.0); H, 3.0 (3.1%). IR (KBr, cm⁻¹): $\nu_{\text{as}}(\text{COO})$, 1675, 1598, 1571, $\nu_{\text{s}}(\text{COO})$, 1403. ¹³C NMR (D₂O, ppm): 185.8 (α -CO₂), 184.4 (β -CO₂), 182.3 (γ -CO₂), 79.3 ($\equiv\text{COH}$), 48.8 ($-\text{CH}_2\text{CO}_2$), 38.1 ($\text{CH}_2-\text{CH}_2\text{CO}_2$), 35.0 ($-\text{CH}_2\text{CH}_2\text{CO}_2$) ppm.

Transformations of 1 to 2. Compound **1** (0.100 g) was suspended in a water–ethanol (1:2 in volume) solution. The pH of the mixture was 5.1. Dark green crystals separated from the green solution when the solvent was slowly evaporated over two weeks to give **2** in quantitative yield. The compound was identified by IR spectra, XRD patterns, and also unit cell dimensions.

X-Ray Structure Determination. Crystals of **1**–**5** in oil were analyzed with a Bruker Smart Apex CCD area detector diffractometer or an Oxford Gemini S Ultra system with graphite monochromate Cu K α radiation ($\lambda = 1.54180$ Å) or Mo K α ($\lambda = 0.71073$ Å) radiation at 173 K. The data were corrected for absorption by using the SADABS program.¹⁸ The structures were primarily solved by SHELXS in the WinGX program¹⁹ and refined by full-matrix least-squares procedures with anisotropic thermal parameters for all of the nonhydrogen atoms with SHELXL-97.²⁰ Hydrogen atoms were located from a difference Fourier map and refined isotropically; they were omitted for clarity in the displayed figures, except for **5**.

- (9) Holland, P. L. In *Comprehensive Coordination Chemistry II*; McCleverty, J. A., Meyer, T. J., Eds.; Elsevier Pergamon: New York, 2004, Vol. 8; pp 586–591.
- (10) (a) Durrant, M. C. *Biochemistry* **2002**, *41*, 13934–13945. (b) Seefeldt, L. C.; Dance, I. G.; Dean, D. R. *Biochemistry* **2004**, *43*, 1401–1409. (c) Zhou, Z. H.; Zhao, H.; Tsai, K. R. *J. Inorg. Biochem.* **2004**, *98*, 1787–1794.
- (11) (a) Grönberg, K. L. C.; Gormal, C. A.; Durrant, M. C.; Smith, B. E.; Henderson, R. A. *J. Am. Chem. Soc.* **1998**, *120*, 10613–10621. (b) Tsai, K. R.; Wan, H. L. *J. Cluster Sci.* **1995**, *6*, 485–501.
- (12) Zhou, Z. H.; Wan, H. L.; Hu, S. Z.; Tsai, K. R. *Inorg. Chim. Acta* **1995**, *237*, 193–197.
- (13) Zhou, Z. H.; Yan, W. B.; Wan, H. L.; Tsai, K. R.; Wang, J. Z.; Hu, S. Z. *J. Chem. Crystallogr.* **1995**, *25*, 807–811.
- (14) Zhou, Z. H.; Zhang, H.; Jiang, Y. Q.; Lin, D. H.; Wan, H. L.; Tsai, K. R. *Trans. Met. Chem.* **1999**, *24*, 605–609.
- (15) Zhou, Z. H.; Deng, Y. F.; Cao, Z. X.; Zhang, R. H.; Chow, Y. L. *Inorg. Chem.* **2005**, *44*, 6912–6914.
- (16) Zhou, Z. H.; Hou, S. Y.; Cao, Z. X.; Tsai, K. R.; Chow, Y. L. *Inorg. Chem.* **2006**, *46*, 8447–8451.

- (17) Chen, H. B.; Chen, L. Y.; Huang, P. Q.; Zhang, H. K.; Zhou, Z. H.; Tsai, K. R. *Tetrahedron* **2007**, *63*, 2148–2152.
- (18) SADABS; University of Göttingen: Göttingen, Germany, 1997.
- (19) Farrugia, L. J. *J. Appl. Crystallogr.* **1999**, *32*, 837–838.
- (20) Sheldrick, G. M. *SHELXL97*; *SHELXS97*; University of Göttingen, Göttingen, Germany, 1997.

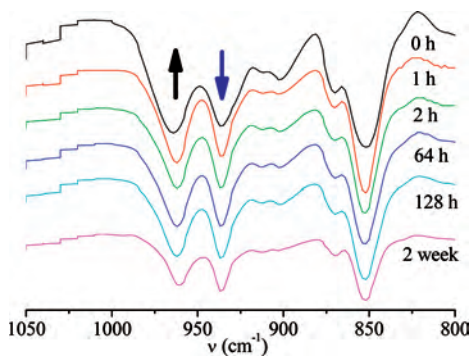


Figure 1. Qualitative IR tracing of the conversion from $[\text{V}_2\text{O}_3(\text{phen})_3(\text{Hcit})] \cdot 5\text{H}_2\text{O}$ (**1**) to $[\text{V}_2\text{O}_3(\text{phen})_3(\text{Hcit})_2(\text{phen})_3\text{O}_3\text{V}_2] \cdot 12\text{H}_2\text{O}$ (**2**) at different times.

Crystal data for **1**: $\text{C}_{42}\text{H}_{39}\text{N}_6\text{O}_{15}\text{V}_2$, $M = 969.67$, triclinic, space group $P\bar{1}$, $a = 12.5702(4)$, $b = 13.5289(6)$, $c = 14.1029(6)$ Å, $\alpha = 73.634(4)$, $\beta = 82.865(3)$, $\gamma = 72.525(4)^\circ$, $V = 2192.9(2)$ Å³, $D_c = 1.469$ g/cm³, $Z = 2$, $R_1 = 0.071$, $wR_2 = 0.239$. Crystal data for **2**: $\text{C}_{84}\text{H}_{82}\text{N}_{12}\text{O}_{32}\text{V}_4$, $M = 1975.38$, triclinic, space group $P\bar{1}$, $a = 13.0831(5)$, $b = 13.0996(4)$, $c = 14.8791(5)$ Å, $\alpha = 101.442(3)$, $\beta = 105.709(3)$, $\gamma = 115.186(3)^\circ$, $V = 2072.5(1)$ Å³, $D_c = 1.583$ g/cm³, $Z = 1$, $R_1 = 0.031$, $wR_2 = 0.096$. Crystal data for **3**: $\text{C}_{43}\text{H}_{44}\text{Cl}_1\text{N}_6\text{O}_{16}\text{V}_2$, $M = 1038.17$, triclinic, space group $P\bar{1}$, $a = 12.9695(8)$, $b = 13.6195(8)$, $c = 15.4979(9)$ Å, $\alpha = 71.586(5)$, $\beta = 78.905(5)$, $\gamma = 63.745(6)^\circ$, $V = 2324.9(2)$ Å³, $D_c = 1.483$ g/cm³, $Z = 2$, $R_1 = 0.059$, $wR_2 = 0.177$. Crystal data for **4**: $\text{C}_{66}\text{H}_{68}\text{N}_8\text{O}_{28}\text{V}_4$, $M = 1625.04$, triclinic, space group $P\bar{1}$, $a = 8.0818(9)$, $b = 13.932(2)$, $c = 15.770(2)$ Å, $\alpha = 113.305(2)$, $\beta = 93.113(2)$, $\gamma = 91.559(2)^\circ$, $V = 1626.0(3)$ Å³, $D_c = 1.660$ g/cm³, $Z = 1$, $R_1 = 0.94$, $wR_2 = 0.198$. Crystal data for **5**: $\text{C}_7\text{H}_9\text{O}_8\text{Na}_3$, $M = 290.11$, triclinic, space group $P\bar{1}$, $a = 5.8041(3)$, $b = 8.0920(5)$, $c = 10.9032(8)$ Å, $\alpha = 80.153(6)$, $\beta = 82.600(5)$, $\gamma = 87.431(5)^\circ$, $V = 500.21(5)$ Å³, $D_c = 1.926$ g/cm³, $Z = 2$, $R_1 = 0.030$, $wR_2 = 0.069$.

Results and Discussion

The reaction of vanadium pentoxide with citric or homocitric acid in the presence of 1,10-phenanthroline in an aqueous ethanol solution is delicately sensitive to pH adjustment, as demonstrated by a digital pH monitor. Excess citrate and a lesser amount of 1,10-phenanthroline are needed for the completeness of the reaction. At pH 4.0, a dimeric mixed-valence complex $[\text{V}_2\text{O}_3(\text{phen})_3(\text{Hcit})] \cdot 5\text{H}_2\text{O}$ (**1**) was isolated as dark green crystals in high yield. At pH 5.0–6.0, however, a tetrameric complex, $[\text{V}_2\text{O}_3(\text{phen})_3(\text{Hcit})_2(\text{phen})_3\text{O}_3\text{V}_2] \cdot 12\text{H}_2\text{O}$ (**2**), was obtained as dark green crystals. The relation was demonstrated by the conversion of **1**, dissolving in a water–ethanol solution from which **2** was deposited quantitatively. As shown in Figure 1, the IR patterns of **1** and **2** are very similar. However, the frequency of V=O vibration around 950 cm⁻¹ could be served as a probe for the reaction. IR tracing of the reaction product from the solution shows that the conversion takes place in the early stage. The switch from an intramolecular bond in **1** to an intermolecular hydrogen bond of the citrate ion in **2** is interesting. Complex **1** could be quantitatively changed into **2** after two weeks in a water–ethanol solution, as further proved by bulk XRD measurements in Figure S1 (Supporting Information). This,

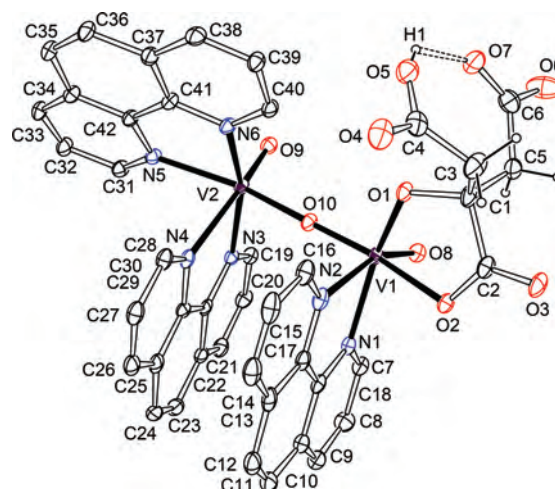


Figure 2. The ORTEP plot of $[\text{V}_2\text{O}_3(\text{phen})_3(\text{Hcit})] \cdot 5\text{H}_2\text{O}$ (**1**) at the 20% probability level. Hydrogen atoms of phenanthroline groups were omitted for clarity.

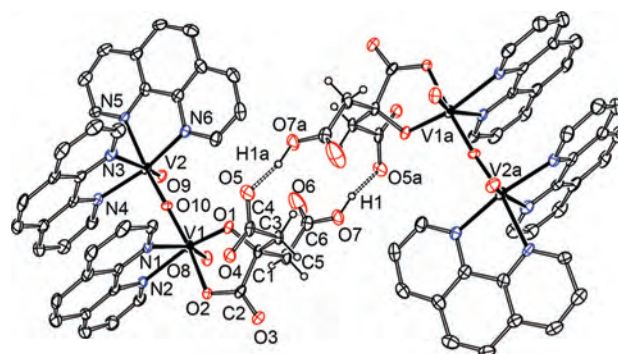
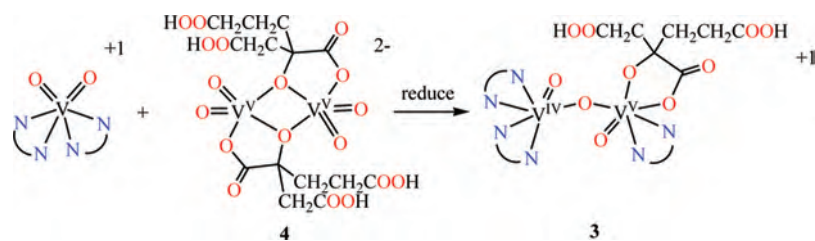


Figure 3. The ORTEP plot of $[\text{V}_2\text{O}_3(\text{phen})_3(\text{Hcit})_2(\text{phen})_3\text{O}_3\text{V}_2] \cdot 12\text{H}_2\text{O}$ (**2**) at the 30% probability level. Hydrogen atoms of phenanthroline groups were omitted for clarity.

in turn, reveals the stability of tetramer **2**, which is experimentally demonstrated in a solid.

Complex **1** is shown to be stabilized by strong intramolecular hydrogen bonding (Figure 2), whereas the formation of tetramer **2** is enforced by strong intermolecular hydrogen bonding (Figure 3). This is eventually substantiated by X-ray structures (vide infra). The detail crystallization processes is not clear at this stage, but it is the fact that, at pH 4.0, monomer **1** crystallized faster.

The reaction of vanadate and racemic homocitrate, both as potassium salts, in the presence of 1,10-phenanthroline at pH 2.5 gave protonated homocitrato vanadate(V/IV) $[\text{V}_2\text{O}_3(\text{phen})_3(\text{R,S-H}_2\text{homocit})]\text{Cl} \cdot 6\text{H}_2\text{O}$ (**3**) as dark green crystals (Scheme 1). In the synthesis of **3**, yellow solid **4** could be obtained in a small amount as an intermediate, which redissolved to form the dark green solid **3** as the final product. X-ray structural analysis shows that the precursor $[\text{VO}_2(\text{phen})_2]_2[\text{V}_2\text{O}_4(\text{R,S-H}_2\text{homocit})_2] \cdot 4\text{H}_2\text{O} \cdot 2\text{C}_2\text{H}_5\text{OH}$ (**4**) is an adduct of the diphenanthroline dioxovanadium cation and dihydrogen homocitrato dioxovanadium anion. The cation diphenanthroline dioxovanadate(V) $[\text{V}^{\text{VO}_2}(\text{phen})_2]^+$ is a direct reaction product of vanadate(V) and the phenanthroline ligand, which is easily reduced to $[\text{V}^{\text{IV}}\text{O}_2(\text{phen})_2]$.²¹ The reduced $[\text{V}^{\text{IV}}\text{O}_2(\text{phen})_2]$ unit might be used as a reactant for the further formation of mixed-valence complex **3**, where

Scheme 1. Transformation of Homocitrato Vanadate(V) to Mixed-Valence Homocitrato Vanadium Complex

the $V_2O_3^{3+}$ core can be viewed as a complex between the donor $V^VO_2^+$ and the acceptor $V^{IV}O_2^{2+}$. The anion structure $[V_2O_4(R,S\text{-}H_2\text{homocit})_2]^{2-}$ of **4** is similar to that found in $K_2[V_2O_4(R,S\text{-}H_2\text{homocit})_2] \cdot 6H_2O$, as shown in Figure S2 (Supporting Information),²² which is a reaction product of vanadate and homocitrate containing a V_2O_4 unit. The homocitrate dianion in **4** bidentately coordinates to the vanadium atom through α -carboxy and the α -alkoxy groups, where the latter acts as a bridging group. A detailed reaction mechanism for the formation of mixed-valence complex **3** is under further study.

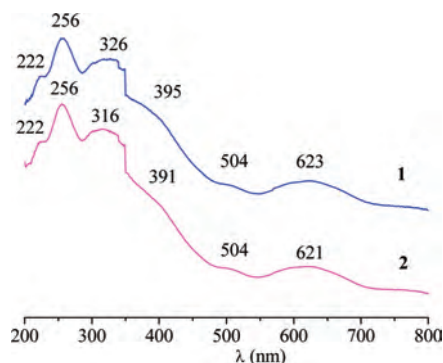
A racemic homocitrate solution was obtained by dissolving the known homocitric acid lactone in aqueous potassium hydroxide and had a pH 10.6. This is proved by the isolation of sodium homocitrate $Na_3(H\text{homocit}) \cdot H_2O$. All of the isolated citrate and homocitrato mixed-valence vanadium-(V/IV) complexes **1**–**3** are insoluble in water and ethanol and slightly soluble in the mixed solvent of water–ethanol.

Vanadium citrate complexes such as the dioxovanadates(V) $[VO_2(H\text{cit})]_2^{2-}$ (**6**),^{13,23,24} $[VO_2(H\text{cit})]_2^{4-}$ (**7**),^{14,25,26} and $[VO_2(\text{cit})]_2^{6-}$ (**8**)^{12,26,27} and vanadyl citrate complexes of $[V_2O_2(H\text{cit})(\text{cit})]_2^{3-}$ (**10**, **11**)^{28,29} and $[VO(\text{cit})]_2^{4-}$ (**12**)^{12,30,31} have been reported. The homocitrato dioxovanadate(V), $K_2[V_2O_4(R,S\text{-}H_2\text{homocit})_2] \cdot 6H_2O$ (**9**), is known to mimic an early mobilized precursor in the synthesis of the V-nitrogenase cofactor.²² These compounds have $V_2(V)O_4$ and $V_2(IV)O_2$ cores, while the citrate or homocitrate group binds directly to the two vanadium atoms through its α -alkoxy group. Previously, in the introduction of the 2,9-dimethyl-1,10-phenanthroline ligand, the *N*-heterocycle group

served as a counteranion in the formation of the vanadyl citrate complex.²⁹ The methyl substituents are unsuitable for the coordination. In fact, the present study shows that 1,10-phenanthroline without a methyl substituent group is an appropriate chelating entity for the synthesis of the mixed ligand complexes **1**–**3**.

The crystal structures of **1** and **2** show a *cis*-oxo- V_2O_3 unit along with a bent oxo bridge [172.2(3) and 160.3(1)°] in Figures 1 and 2, respectively. The $V1 \cdots V2$ distances are on the order of 3.5 Å, a distance that implicates a weak interaction between two metal centers. The vanadium atom is six-coordinate in a distorted octahedral geometry. The citrate group chelates to one vanadium atom as a bidentate ligand via its α -alkoxy and carboxy oxygen atoms, whereas the other β -carboxy and β -carboxylic acid groups are free. The free groups participate in a very strong intramolecular hydrogen bond [**1**, $O5 \cdots O7 = 2.46(1)$ Å] and intermolecular hydrogen bond [**2**, $O5a \cdots O7 = 2.487(4)$ Å]. The $O \cdots O$ distances are short in comparison with the bond found in, for example, dimeric acetic acid (2.68 Å).³² Here, the β -carboxy and β -carboxylic acid groups are involved in the formation of an intramolecular hydrogen bond in **1**. In a previous quantum-mechanical computation and a model suggestion, the γ -carboxy group of *R*-homocitrate is proposed as undergoing intramolecular hydrogen bonding with the imidazole ligand on Mo, while the β -carboxy group of the citrate ligand is not.¹¹

Compound **1** exhibits photoinstability under UV radiation, as shown in Figure S3 (Supporting Information). This is inconsistent with the strong absorption of solid **1** in the UV diffused reflectance spectra in Figure 4. Bands in the 550–800 nm region are assigned to a d–d transition, and the bands in the 350–550 nm region can be assigned to

**Figure 4.** Diffuse reflectance spectra of solid $[V_2O_3(\text{phen})_3(\text{Hcit})] \cdot 5H_2O$ (**1**) and $[V_2O_3(\text{phen})_3(\text{Hcit})_2(\text{phen})_3O_3V_2] \cdot 12H_2O$ (**2**).

- (21) Qi, Y. J.; Yang, Y. L.; Cao, M. H.; Hu, C. W.; Wang, E. B.; Hu, N. H.; Jia, H. Q. *J. Mol. Struct.* **2003**, *648*, 191–201.
- (22) Wright, D. W.; Chang, R. T.; Mandal, S. K.; Armstrong, W. H.; Orme-Johnson, W. H. *J. Biol. Inorg. Chem.* **1996**, *1*, 143–151.
- (23) Wright, D. W.; Humiston, P. A.; Orme-Johnson, W. H.; Davis, W. M. *Inorg. Chem.* **1995**, *34*, 4194–4197.
- (24) Tsaramyrsi, M.; Kavousanaki, D.; Raptopoulou, C. P.; Terzis, A.; Salifoglou, A. *Inorg. Chim. Acta* **2001**, *320*, 47–59.
- (25) Kaliva, M.; Giannadaki, T.; Salifoglou, A.; Raptopoulou, C. P.; Terzis, A. *Inorg. Chem.* **2002**, *41*, 3850–3858.
- (26) Kaliva, M.; Raptopoulou, C. P.; Terzis, A.; Salifoglou, A. *J. Inorg. Biochem.* **2003**, *93*, 161–173.
- (27) Aureliano, M.; Tiago, T.; Gândara, R. M. C.; Sousa, A.; Moderno, A.; Kaliva, M.; Salifoglou, A.; Duarte, R. O.; Moura, J. J. G. *J. Inorg. Biochem.* **2005**, *99*, 2355–2361.
- (28) Tsaramyrsi, M.; Kaliva, M.; Salifoglou, A.; Raptopoulou, C. P.; Terzis, A.; Tangoulis, V.; Giapintzakis, J. *Inorg. Chem.* **2001**, *40*, 5772–5779.
- (29) Burojevic, S.; Shweky, I.; Bino, A.; Summers, D. A.; Thompson, R. C. *Inorg. Chim. Acta* **1996**, *251*, 75–79.
- (30) Rehder, D.; Pessoa, J. C.; Geraldes, C. F. G. C.; Castro, M. M. C. A.; Kabanos, T.; Kiss, T.; Meier, B.; Micera, G.; Pettersson, L.; Rangel, M.; Salifoglou, A.; Turel, I.; Wang, D. R. *J. Biol. Inorg. Chem.* **2002**, *7*, 384–396.
- (31) Velayutham, M.; Varghese, B.; Subramanian, S. *Inorg. Chem.* **1998**, *37*, 1336–1340.

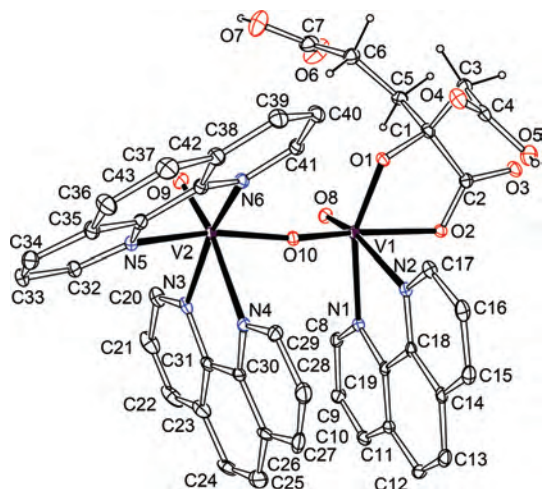


Figure 5. The ORTEP plot of $[V_2O_3(phen)_3(R,S-H_2homocit)]Cl \cdot 6H_2O$ (**3**) at the 30% probability level. Hydrogen atoms of phenanthroline groups were omitted for clarity.

metal-to-ligand charge transfer. The bands below 350 nm region should be the $\pi-\pi$ transition.³³

The V–O distances in **1** and **2** vary systematically according to the bond types in Table S1 (Supporting Information); the short V=O distances are in agreement with the double-bond character. The bond distances for the VOV bridge are unequal but fall within the range found for the oxo-bridged, mixed-valence complex, $(NH_4)_3[V_2O_3(nta)_2] \cdot 3H_2O$.³⁴ Bond valence calculations give valences of 5.0 and 4.3 for **1** and 5.0 and 4.3 for **2**.³⁵ The assignments are supported by an XPS analysis of V2p as shown in Figure S4 of the Supporting Information. The peaks at 516 and 523 eV correspond to vanadium 2p_{3/2} and 2p_{1/2} in the oxidation states of V and IV.³⁶ Moreover, the X-band EPR spectra of VO(IV/V) mixed-valence complexes **1** and **2** were recorded in the solid state at 100, 150, 200, and 250 K, as shown in Figures S5a and S5b (Supporting Information). The EPR spectra of **1** and **2** exhibit one broad band centered on $g = 1.991$ and $g = 1.995$, respectively, without a resolved hyperfine structure. In particular, the hyperfine coupling around the ^{51}V ($I = 7/2$, $S = 1/2$) nucleus is not observable. The absence of vanadium's hyperfine coupling is common in the solid state and is attributed to the simultaneous flipping of neighboring electron spin or is due to strong exchange interactions, which average out the interaction with the nuclei.³⁷

In homocitrato complex $[V_2O_3(phen)_3(R,S-H_2homocit)] \cdot Cl \cdot 6H_2O$ (**3**), the molecular structure is similar to those of **1** and **2**, see Figure 5. The V(1)–O(10) distance [1.713(4) Å] is much shorter than the V(2)–O(10) distance [1.884(4) Å],

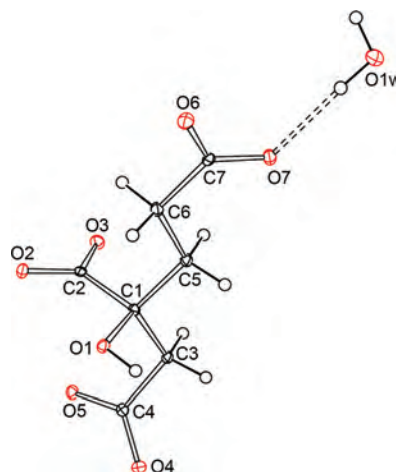


Figure 6. The ORTEP plot of $Na_3(Hhomocit) \cdot H_2O$ (**5**) at the 30% probability level.

which implies an unsymmetric configuration. The bond valence summaries are 5.0 and 4.4 for V1 and V2, respectively.³⁵ The homocitrate ion acts as a bidentate ligand through its α -alkoxy and α -carboxy groups, leaving the β -carboxylic and γ -carboxylic acid groups free. The V–O distance [α -alkoxy 1.858(4) Å] is comparable to those of **1** and **2** but much shorter than that of $K_2[V_2O_4(R,S-H_2homocit)_2] \cdot 6H_2O$ (**9**) [1.980(8)_{av} Å],²² while the V–O distance [α -carboxy, 2.085(4) Å] is longer than that of **9** [1.959(8)_{av} Å]. This should be the result of the strong trans influence of the short V(1)–O(10) bond. Moreover, the discrete structure of complex **3** is linked by the weak hydrogen bonding between O(5)–Cl(1) and O(7)–Cl(1) [3.004(5), 2.982(5) Å]; the latter is from the γ -carboxy group of the homocitrate ligand. The hydrogen bond from the γ -carboxy group could also be seen from the structural analysis of homocitrato salt **5**, which forms a strong hydrogen bond between the γ -carboxy group and the water molecule [2.763(1) Å], as shown in Figure 6. Moreover, the anion bridged core of **4** is defined by the O(1)–V(1)–O(1a) [71.2(3)°] and the V(1)–O(1)–V(1a) [108.8(3)°] angles. This is similar to the 71.6(3)° and 108.4(3)° given for **9**. The V–O distances [V–O_{alkoxy} = 1.968(6)_{av}, V–O_{carboxy} = 1.937(5) Å] of complex **4** are the shortest bonds among the citrate and homocitrato vanadates(V). The hydrogen bond between the γ -carboxy group and the water molecule [2.562(9) Å] in **4** is the most strongest in the reported homocitrato complexes.^{16,22} The transformation of **4** to **3** shows that bulky conjugated phenanthroline is useful for the formation of bidentate homocitrate coordinated in only one vanadium center, which avoids the formation of a bridging α -alkoxy group.

Obvious downfield shifts of ^{13}C NMR spectra in **5** are observed compared with those of homocitric acid γ -lactone, except for that of α -hydroxy carbon in D₂O. For example, both β - and γ -carboxy carbons of **5** show large downfield shifts of $\Delta\delta$ 6.9 and 6.8 ppm, respectively, arising from the basic medium and delactonization. The α -carboxy carbon has somewhat small downfield shifts of $\Delta\delta$ 3.1 ppm. Other peaks of methylene carbons also show downfield shifts in general. This is a clear indication for the hydrolysis of the

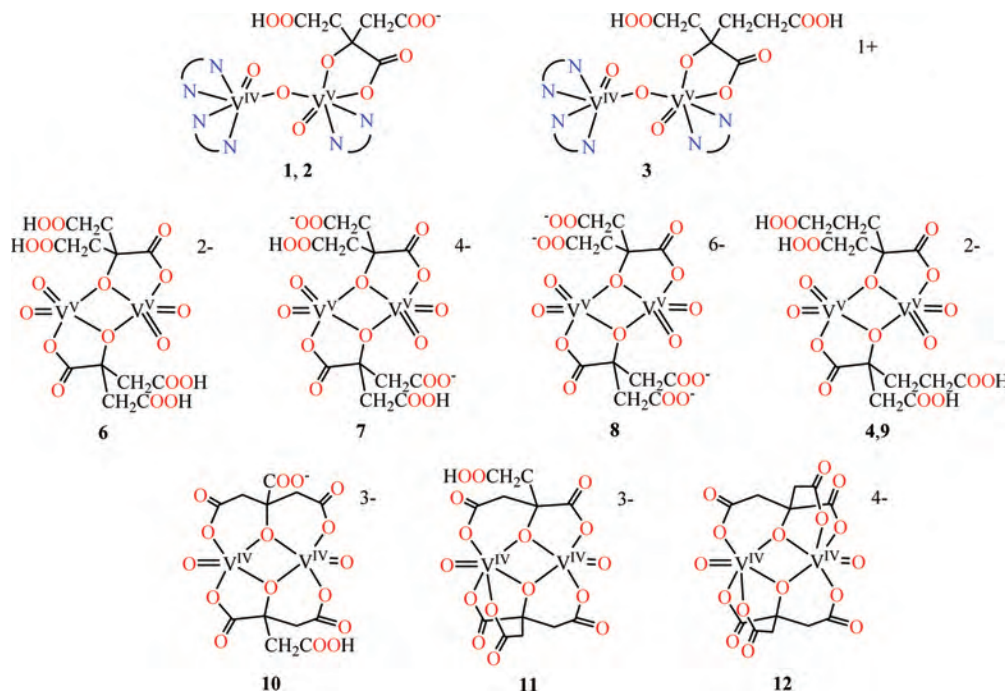
- (32) Rodríguez-Cuamatzi, P.; Arillo-Flores, O. I.; Bernal-Uruchurtu, M. I.; Höpfl, H. *Cryst. Growth Des.* **2005**, *5*, 167–175.
 (33) Kovalevsky, A. Y.; Gembicky, M.; Novozhilova, I. V.; Coppens, P. *Inorg. Chem.* **2003**, *42*, 8794–8802.
 (34) Nishizawa, M.; Hirotsu, K.; Ooi, S.; Saito, K. *Chem. Comm.* **1979**, 707.
 (35) Brown, I. D.; Altermatt, D. *Acta Crystallogr., Sect. B* **1985**, *41*, 244–247.
 (36) Silversmit, G.; Depla, D.; Poelman, H.; Marin, G. B.; De Gryse, R. *J. Electron Spectrosc. Relat. Phenom.* **1991**, *57*, 189–197.
 (37) Bencini, A.; Gatteschi, D. *EPR of Exchange Coupled Systems*; Springer Verlag: New York, 1990.

Table 1. ¹³C NMR Spectral Data (in ppm, D₂O or CD₃OD) of Homocitric Acid γ -Lactone and Homocitrate Na₃(Hhomocit)·H₂O (5)^a

compound	(¹³ C=O)	(CO ₂) _{α}	(CO ₂) _{β}	(CO ₂) _{γ}	(=CH ₂)
homocitric acid γ -lactone (D ₂ O)	87.0	182.7	177.5	175.8	44.0,33.7,30.3
homocitrate 5 (D ₂ O)	79.3(−7.7)	185.8(3.1)	184.4(6.9)	182.3(6.8)	48.8(4.8),38.1(4.4),35.0(4.7)
homocitric acid γ -lactone (CD ₃ OD) ¹⁷	84.7	178.77	174.1	172.48	42.1,32.3,28.7

^a $\Delta\delta$ values are given in parentheses.**Table 2.** Comparisons of V–O Distances (Å) in Citrato and Homocitrate Vanadium Complexes (neo = 2,9-Dimethyl-1,10-phenanthroline)

complex	V–O (Å) (α -alkoxy)	V–O (Å) (α -carboxy)	ref
[V ₂ O ₃ (phen) ₃ (Hcit)]·5H ₂ O (1)	1.851(4)	2.082(4)	this work
[V ₂ O ₃ (phen) ₃ (Hcit) ₂ (phen) ₃ O ₃ V ₂]·12H ₂ O (2)	1.858(1)	2.072(1)	this work
[V ₂ O ₃ (phen) ₃ (R,S-H ₂ homocit)]Cl·6H ₂ O (3)	1.858(4)	2.085(4)	this work
Average	1.856(4)	2.080(4)	
K ₂ [V ₂ O ₄ (H ₂ cit) ₂]·4H ₂ O (6)	1.986(2) _{av}	1.980(3)	13, 23
Na ₂ K ₂ [V ₂ O ₄ (Hcit) ₂]·9H ₂ O (7)	1.984(4) _{av}	1.979(4) _{av}	14, 24–26
K ₂ (NH ₄) ₄ [V ₂ O ₄ (cit) ₂]·6H ₂ O (8)	1.983(2) _{av}	1.981(2)	12, 26, 27
K ₂ [V ₂ O ₄ (R,S-H ₂ homocit) ₂]·6H ₂ O (9)	1.980(8) _{av}	1.959(8) _{av}	22
[VO ₂ (phen) ₂][V ₂ O ₄ (R,S-H ₂ homocit) ₂]·4H ₂ O·2C ₂ H ₅ OH (4)	1.968(6) _{av}	1.937(5)	this work
Average	1.980(8)	1.967(8)	
K ₃ [V ₂ O ₂ H(cit) ₂]·7H ₂ O (10)	1.976(5) _{av}	1.981(6)	28
(Hneo) ₃ [V ₂ O ₂ H(cit) ₂]·4H ₂ O (11)	1.984(4) _{av}	2.137(4) _{av}	29
Na ₄ [V ₂ O ₂ (cit) ₂]·6H ₂ O (12)	2.089(2) _{av}	2.038(2)	12, 30, 31
Average	2.016(5)	2.052(6)	
VFe ₇ S ₉ X(homocit)(S-cys)(N-His)		2.15	38

Scheme 2. Typical Coordination Modes of Citrate and Homocitrate with Vanadium(V,IV): Mixed-Valence Citrato and Homocitrate Vanadate(V/IV), **1**–**3**; Citrato and Homocitrate Vanadate(V), **6**–**9**^[12–14, 23–27]; and Vanadyl Citrate, **10**–**12**^[12,28–31]

γ -lactone. Moreover, the downfield shifts (2–3 ppm) of ¹³C NMR spectra in the strong polar solvent D₂O are observed compared with that of CD₃OD. Table 1 gives a ¹³C NMR data comparison between homocitric acid γ -lactone and sodium homocitrate **4** in D₂O and CD₃OD solvents. The ¹³C spectra of homocitrate acid γ -lactone and sodium homocitrate **4** are shown in Figures S6 and S7 (Supporting Information).

Furthermore, attempts to isolate a similar citrato complex of [V₂O₃(phen)₃(H₂cit)]·Cl were unsuccessful. This may be related to the formations of the species with very strong hydrogen bonds in **1** and **2**. On the other hand, no isolation of [V₂O₃(phen)₃(Hhomocit)] is attributed temporarily to the equilibrium between homocitric acid γ -lactone and homocitrate in a weak acidic solution and the dissociation of

homocitrate vanadate in solution. The present isolations of complexes **1**–**3** give a new class of citrato and homocitrate vanadates in different oxidation states, as shown in Scheme 2.

In the mixed-valence dimeric citrato vanadates (V/IV), the bond distances of α -alkoxy to vanadium are shorter than those of vanadates(V) and vanadyl citrates, see Table 2. The latter ones are strongly influenced by the bridging mode coordination in the V₂O₄ or V₂O₂ units. However, the differences between V–O (α -carboxy) distances (1.979–2.137 Å) are smaller, being close to the V–O distance (2.15 Å) in homocitrate FeVco.³⁸ The short distances of V–O (α -alkoxy) in compounds **1**–**3** are worthy of note, which

indicates strong binding of the α -alkoxy group to the vanadium atom in the high oxidation state.

Conclusions

There is sufficient evidence to show that the vanadyl citrate engages in tridentate and tetradentate coordination via the α -alkoxy, α -carboxy, and β -carboxy groups in the complexes $K_3[V_2O_2H(cit)_2] \cdot 7H_2O$ (**10**), $(Hneo)_3[V_2O_2H(cit)_2] \cdot 4H_2O$ (**11**), and $Na_4[V_2O_2(cit)_2] \cdot 6H_2O$ (**12**).^{12,28–31} The present formation of symmetric and unsymmetric bidentate citrato and homocitrato vanadate **1**–**4** could be related to the bidentate homocitrato FeVco in nitrogenase, which shows a resemblance in coordination mode. Although, a detailed structure of the homocitrato vanadate of FeVco is unknown.³⁸ It is also noted that a large gap exists between the homocitrato vanadate in the natural cofactor and in the current model molecules. The present structural examples show that citrate and homocitrato mixed-valence complexes feature bidentate citrato or homocitrato groups that chelate to one vanadium atom through its α -alkoxy and α -carboxy oxygen atoms, while the other β - or γ -carboxylic acid groups are free. The bond distances [$2.080(4)_{av}$ Å] of α -carboxy groups to vanadium in **1**–**3** are close to that of homocitrato to FeVco (2.15 Å), while those [$1.856(4)_{av}$ Å] of α -alkoxy groups to

vanadium are shorter (2.15 Å). This is attributed to a strong coordination of vanadium in the mixed-valence citrate and homocitrato vanadium^{V/IV} complexes. The chemical conversion of mixed-valence vanadium citrate complexes suggests that the citrate complex **1** with an intramolecular hydrogen bond could be converted to the tetrameric form **2** with strongly interacting hydrogen bonds in the solid. Moreover, the β -carboxy group in the citrate ligand is also effective and should be noted in the further consideration of intramolecular hydrogen bonds in the vanadium citrate complex, including the biomolecular chemistry of the homocitrato–FeVco in nitrogenase.

Acknowledgment. Financial support provided by the National Science Foundation of China (20571061) and the Ministry of Science & Technology (2005CB221408) is gratefully acknowledged. We thank Professor S. W. Ng for stimulating discussion and the reviewers for their very constructive suggestions to update the paper.

Supporting Information Available: IR, XPS, EPR, XRD, ¹³C NMR, and the image of the conversion between **1** and **2**; tables of crystal and refinement data; atomic positions and displacement parameters; anisotropic displacement parameters; and bond lengths and angles in CIF format. This material is available free of charge via the Internet at <http://pubs.acs.org>.

(38) George, G. N.; Coyle, C. L.; Hales, B. J.; Cramer, S. P. *J. Am. Chem. Soc.* **1988**, *110*, 4057–4059.

IC800553P